Proceedings of the 28th IEEE
EMBS Annual International Conference
New York City, USA, Aug 30-Sept 3, 2006

Analytical Calculation of the Self-Resonant Frequency of Biomedical Telemetry Coils

Zhi Yang, Guoxing Wang, and Wentai Liu

Department of Electrical Engineering, University of California at Santa Cruz, CA 95064

Abstract— **Inductive link is commonly used in biomedical telemetry as a method to wirelessly transmit power and/or data, where coil is very critical to achieve high efficiency. One of the most important but often ignored parameters of the coils is the self-resonant frequency. Due to the fact that the parasitic capacitances are functions of the geometry and winding sequence of the coil, it is very difficult to calculate the self-resonant frequency. The lack of knowledge about the self-resonant frequency greatly limits the design efficiency, especially when the target operating frequency is high, on the order of tens of MHz. This paper presents an analytical model to calculate the self-resonant frequency of multiple-layer coils. A general model of coils to calculate the total parasitic capacitance is given first and then an analytical equation for self-resonant frequency is obtained. The experimental measurement results demonstrate that the equation can accurately predict the self-resonant frequency, therefore can be used for guiding the coil design.**

I. INTRODUCTION

Inductive links are commonly used in biomedical applications for wireless transmission of power and/or data [1], [2]. Coil design is very critical for achieving high efficiency in these links. Frequency related effects, such as skin effect, proximity effect and coil's self-resonance, significantly limit a coil's performance and power efficiency. Many coil designs focus on skin effect and proximity effect [3]-[5], with the goal of improving the quality factor (Q). Nevertheless, most papers assume that the self-resonant frequency is well above the coil's operating frequency. Without careful design, the coil's self-resonant frequency may actually fall below the targeted operating frequency, resulting in less efficiency or even unusable design [6]. Therefore, the self-resonant frequency should be considered at the stage of designing the coil. To the best of our knowledge, however, only a few publications have addressed this problem. A method to calculate the parasitic capacitance between two turns was proposed in [7]. Using the method in [7], an estimation of the self-resonant frequency for single-layer coil has been provided in [8]. Due to the complexity of parasitic capacitive branches in a multiple-layer coil, a quantitative analysis is not available.

The analysis in this paper focuses on general analytical expressions for both multiple-layer and single-layer coils' parasitic capacitances and thus their self-resonant frequencies. Numerical design examples and experimental data are presented, with discussions to increase a coil's self-resonant frequency.

II. COILS IN BIOMEDICAL TELEMETRY

A general structure of a coil is shown in Fig.1. In order to minimize the AC power losses at high frequencies, litz wires, which are constructed of individually insulated strands twisted to a circular shape, are commonly used. By choosing the radius of single strand to be comparable with or even smaller than its skin depth, the AC power losses due to skin effect and proximity effect are reduced [9].

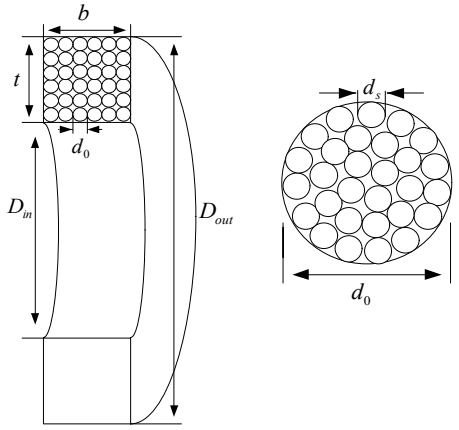

Fig. 1. Multiple-layer litz coil structure and its equivalent circuit.

In Fig.1, t, b, D_{in} and D_{out} represent a coil's thickness, width, inner diameter and outer diameter, respectively. d_0 and d_s are the diameters of a single turn and a single strand.

III. SELF INDUCTANCE CALCULATION

As will be shown in the next section, a coil's self-resonant frequency is related to its self-inductance. The equivalent distributive network of a coil at low frequency is illustrated in Fig. 2.

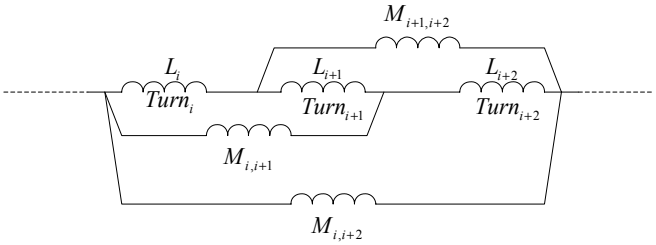

Fig. 2 Equivalent distributive network of a coil at low frequency

The self inductance can be computed as

$$L_{self} = \sum_{i,j} M_{i,j} + \sum_{i} L_i \quad . \tag{1}$$

In Eq.(1), $M_{i,j}$ is the mutual inductance between turn i and turn j. To calculated $M_{i,j}$, the Ralyleigh quadrature formula [11]

is used, due to its accuracy and easy implementation. L_i is the self inductance of a single turn and is represented as [10]

$$L_i = 0.5\mu_0 D_i \ln(D_i / d_0), \quad (2)$$

where D_i is the average diameter of the conductor loop and d_0 the diameter of a single turn.

IV. SELF-RESONANT FREQUENCY OF LITZ COIL

Self-resonant frequency sets an upper limit for the coil's operation frequency and should be considered as an important design parameter. Nevertheless, the estimation of self-resonant frequencies for multiple-layer coils is very challenging due to the fact that a coil's total parasitic capacitance is strongly affected by the geometry parameters and even the winding sequence as will be shown later. Several studies have been conducted to estimate coils' parasitic capacitance, but are limited to the turn-to-turn parasitic capacitance or the overall parasitic capacitance for single-layer coils [7], [8]. Study on multiple-layer coil has not been done due to the complexity. In this section, an analytical expression to compute the self-resonant frequency of a multiple-layer litz coil is given in section IV-A, followed by numerical calculations of the turn-to-turn parasitic capacitance and design examples in section IV-B and IV-C.

A. Analytical Expression of the Self-Resonant Frequency

An equivalent circuit network for a multiple-layer coil at high frequency is shown in Fig.3.

As illustrated in Fig.3, a coil is modeled as a distributive RCL circuit network. Given that the voltage difference between two strands in the same turn is very small compared with the voltage difference between turns, the parasitic capacitances between strands in the same turn is ignored in the model. Each turn is modeled as one node with unit inductance and AC resistance. Both inductive and capacitive couplings between turns (p and k) are modeled as mutual inductance $M_{p,k}$ and capacitance $C_{p,k}$.

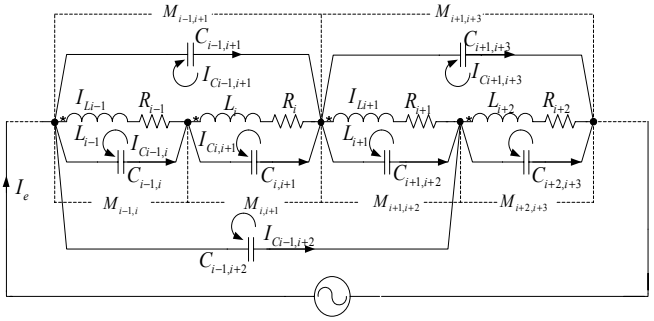

Fig. 3 Distributive equivalent model of a coil. I_{Li} represents the current going through the inductive branch L_i, R_i is the equivalent ESR of the inductive branch L_i, $I_{Cp,k}$ denotes the mesh current through the parasitic capacitance $C_{p,k}$, I_e is the external driving current and $M_{p,k}$ is the mutual inductance between turn p and k.

At a coil's self-resonance, the external driving current I_e reaches its minimum. The corresponding frequency (self-resonant frequency) can be found by solving the network as shown in Fig.3. To obtain a convenient expression of the currents at different branches, the Mesh Theorem [12] is used. Since the number of independent meshes is equal to the number of parasitic capacitances plus one which comes from the external driving circuit, we construct the mesh current based on individual parasitic capacitance. Denoting the mesh current from node p to node k as $I_{Cp,k}$, and the external driving current as I_e, I_{Li} is represented as the sum of the mesh currents and the external driving current

$$I_{Li} = I_e - \sum_{p\le i,k\ge i+1} I_{cp,k} \ . \quad (3)$$

Through the inductive branches, we obtain the voltage difference between node p and node k as

$$V_{p,k} = \sum_{p\le i<k} \omega L_i I_{Li} + \sum_{p\le i<k}\sum_{j\ne i} \omega M_{j,i} I_{Lj} + \sum_{p\le i<k} I_{Li} R_i \ , \quad (4)$$

where L_i is the unit inductance of turn i, $M_{i,j}$ the mutual inductance between turn j and turn i, and R_i the unit ESR of turn i, as shown in Fig.3.

In biomedical applications, a coil's cross-section is typically much smaller than the area of the conductor loop ($b<<D_{out}$, $t<<D_{out}$). Therefore, magnetic field coupling between two turns is very strong. To simplify Eq.(4), assuming that the coupling coefficients between any two turns are 1, thus the flux (Φ_{unit}) going through any individual turn is the same and represented as

$$\begin{aligned}\Phi_{unit} &= \sum_{i=1,N_t} L_i I_{Li} = N_t L_i I_e - L_i \sum_{i=1,N_t}\sum_{p\le i,k\ge i+1} I_{Cp,k} \\ &= N_t L_i I_e - L_i \sum_{p<k} I_{Cp,k}(k-p)\end{aligned} \ , \quad (5)$$

where N_t is the number of turns. Therefore, the voltage difference between node p and node k becomes

$$V_{p,k} = \omega(k-p)\Phi_{unit}\angle 90^o + R_i \sum_{p\le i<k} I_{Li} \ . \quad (6)$$

Alternatively, the voltage difference can also be computed through the capacitive branches as

$$V_{p,k} = I_{Cp,k}\angle -90^o / (\omega C_{p,k}) \ . \quad (7)$$

Eq.(6) and Eq.(7) are combined to give the following expression for the mesh current $I_{Cp,k}$ as

$$I_{Cp,k} = -\omega^2 C_{p,k}(k-p)\Phi_{unit} + \omega R_i C_{p,k}\angle 90^o \sum_{i\in[p,k)} I_{Li} \ . \quad (8)$$

To obtain a direct relationship between the external driving current I_e and the frequency, taking the sum of $(k\text{-}p)$ $I_{Cp,k}$ and the resulting equation is

$$\begin{aligned}\sum_{p<k}(k-p) I_{Cp,k} &= -\omega^2 \Phi_{unit} \sum_{p<k} C_{p,k}(k-p)^2 \\ &\quad + \omega R_i \angle 90^o \sum_{p<k} C_{p,k}(k-p) \cdot \sum_{p\le i<k} I_{Li}\end{aligned} \ . \quad (9)$$

Substituting Eq.(5) into Eq.(9) yields

$$1/(1-\alpha) = \omega^2 L_i \sum_{p<k} C_{p,k}(k-p)^2 - \omega R_i \angle 90^o \sum_{p<k} C_{p,k}(k-p) \ , \quad (10)$$

where $\alpha = N_t I_e / \sum_{p<k} I_{Cp,k}(k-p)$. (11)

The solution to Eq.(10) is

$$\omega = (A \pm B)/G \ , \quad (12)$$

where $A = R_i \angle 90^o \sum_{p<k} C_{p,k}(k-p)$,

$$B = \sqrt{\frac{1}{1-\alpha} 4L_i \sum_{p<k} C_{p,k}(k-p)^2 - R_i^2 [\sum_{p<k} C_{p,k}(k-p)]^2} \ ,$$

and $G = 2L_i \sum_{p<k} C_{p,k}(k-p)^2$.

At the self-resonant frequency of a coil, the external driving current is typically negligible compared with the sum of the mesh currents. Moreover, the ESR of a litz coil is much smaller

than its reactance (opposition to the current flow caused by the inductance). These conditions can be represented as follows:

i). $\alpha \approx 0$.

ii). $N_t R_i \ll L = N_t^2 L_i$.

Using the above conditions, we can further simplify Eq.(12) and find the self-resonant frequency f_{self} as

$$f_{self} = \frac{1}{2\pi\sqrt{LC_{self}}}, \tag{13}$$

where $L = N_t^2 L_i$,

and $C_{self} = \sum_{p<k} C_{p,k}(k-p)^2 / N_t^2$. (14)

In Eq.(14), C_{self} is the total equivalent parasitic capacitance. Eq.(14) implies that a distributive coil model can be simplified as a lumped total capacitance C_{self} in parallel with its inductance when the magnetic field couplings between two turns are strong.

B. Turn-To-Turn Parasitic Capacitance

Eq.(13) and Eq.(14) can be used to calculate the self-resonant frequency of a coil once the parasitic capacitances between any two nodes $C_{p,k}$ are given. In this section, we calculate the turn-to-turn parasitic capacitance given the geometry parameters. The cross section of a multiple-layer coil is shown in Fig.4.

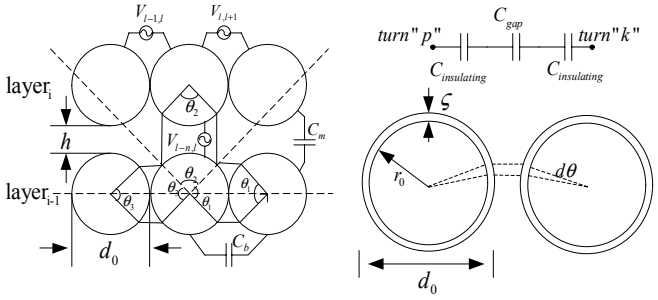

(a) (b)

Fig. 4. Turn-to-turn parasitic capacitance through air gap and insulation layer.

In Fig.4(a), C_m denotes the parasitic capacitance between turns in different layers, C_b the parasitic capacitance between turns in the same layer, and θ_e (e=1,2,3) is the effective angle between two turns. As illustrated in Fig.4(b), turn-to-turn parasitic capacitance is a combination of parasitic capacitances through the insulation layer and the air gap.

The parasitic capacitance contributed by insulting layer per unit angle is calculated as [7]

$$C_{insulate} = \varepsilon_0 \varepsilon_r \pi D_i / \ln[r_0/(r_0 - \varsigma)], \tag{15}$$

where ς is the thickness of the insulation layer, as shown in Fig.4(b), r_0 the radius of a single turn and D_i the average diameter of the conductor loop.

The parasitic capacitance contributed by the air gap per unit angle is approximately computed by

$$C_{gap} = \varepsilon_0 \pi D_i / [2(1-\cos\theta) + h/r_0], \tag{16}$$

where h is the separation between two turns.

As a result, the total parasitic capacitance per unit angle is approximately given as

$$C_t = \frac{0.5 C_{gap} C_{insulate}}{C_{gap} + 0.5 C_{insulate}}. \tag{17}$$

Under the condition that $\varsigma << r_0$, the total parasitic capacitance between two turns is

$$C_{p,k} = \varepsilon_0 \varepsilon_r \int_0^{\theta_e/2} \pi D_i r_0 / [\varsigma + \varepsilon_r r_0 (1-\cos\theta) + 0.5\varepsilon_r h] d\theta, \tag{18}$$

As a first order approximation, we assume that each turn except those on the perimeter of a coil is surrounded by four turns and the effective angles are the same, which means $\theta_1 = \theta_2 = \theta_3 = \theta_e = 90^o$.

C. Design Example

To increase the self-resonant frequency of a coil, one has to decrease either the total parasitic capacitance or the inductance. Generally, the inductance can not be arbitrarily changed, due to other requirements of telemetry. Therefore a more applicable way to increase a coil's self-resonant frequency is to decrease the parasitic capacitance without changing the inductance. An effective way to decrease its parasitic capacitance is to increase the distance between turns. As will be shown later in this section, the winding sequence of the turns of a coil also affects the effective self-resonant frequency. To demonstrate this, an illustration of different coil structures with the same number of turns is shown in Fig.5.

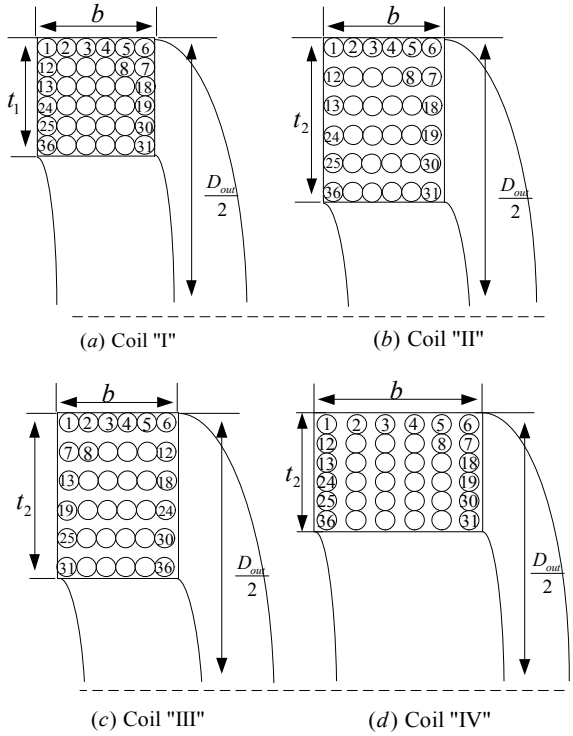

Fig. 5. Coil's cross-sections. (a) Tightly wound litz coil with normal winding sequence. (b) Loosely wound litz coil with normal winding sequence and separation between layers. (c) Loosely wound litz coil with different winding sequence and separation between layers. (d) Loosely wound litz coil with normal winding sequence and separation between turns in the same layer.

In Fig.5, the numbers in the coils indicate the winding sequences. All four coils have the same outer diameter. Coil "I" "II", and "III" have the same width. Coil "II", "III" and "IV" have the same area efficiency. Coil "II" and coil "III" have extra separations between two layers. Coil "III" has different

winding sequence. Coil "IV" has separation between turns in the same layer instead of having separation between layers.

According to Eq.(14), a general expression of the total parasitic capacitance for coil "I", "II" and "IV" is

$$C_{self} = C_b(l-1)m/N_t^2 + C_m \sum_{i=(1,l)} (2i-1)^2 (m-1)/N_t^2, \qquad (19)$$

where C_b is the parasitic capacitance between two nearby turns in the same layer and C_m the parasitic capacitances between different layers, l is the number of turns per layer, and m is the number of layers in the winding.

Due to a different winding sequence, the total parasitic capacitance for coil "III" is expressed as

$$C_{self} = C_b(l-1)m/N_t^2 + C_m l^3 (m-1)/N_t^2. \qquad (20)$$

To obtain a coil's self-resonant frequency, the turn-to-turn parasitic capacitances (C_m, C_b) are required and computed for coils with different winding structures using Eq.(18).

The total parasitic capacitances and self-resonant frequency of coil "I-IV" are calculated using D_{out}=*3cm*, r_0=*100um*, ς~*3um*, and ε_r~*3um*. The results are given in Table I.

Table I
Parasitic capacitance, inductance and self-resonant frequency of coil "I", "II", "III" and "IV"

	C_b	C_m	C_{self}	L	f_{self}
Coil "I" $h=0$	15pF	15pF	17pF	85uH	4.1MHz
Coil "II" $h=r_0$	15pF	1.0pF	1.5pF	77uH	15MHz
Coil "III" $h=r_0$	15pF	1.0pF	1.2pF	77uH	17MHz
Coil "IV" $h=r_0$	1.0pF	15pF	16pF	78uH	4.5MHz

As shown in Table I, coils with separation between layers (Coil "II" and "III") have a much higher self-resonant frequency than those without separation between layers (Coil "I" and "IV"). A separation between turns in the same layer, however, does not increase the self-resonant frequency much (Coil "IV"). Coil "II" and "III" have the same geometry properties, except the different winding sequence. This different winding sequence results in ~15% total parasitic capacitance difference, which implies that the winding sequence is also important for achieving high self-resonant frequencies.

Generally, in biomedical applications, there exist strict requirements on a coil's outer diameter and thickness, and the inner diameter of a coil is usually the design parameter left for further optimization. Therefore, a reasonable separation between layers can always be achieved at the cost of a reduced inner diameter.

V. EXPERIMENTAL RESULTS

To verify the proposed theory, we wound several coils with litz wire AWG 44, and measured their self-resonant frequencies. For convenience, all the coils are tightly wound, as illustrated in Fig.4(a). The parameters of different coils are given in Table II. Also included are measured self-resonant frequencies and the theoretically predicted results calculated according to Eqs. (1), (13), (18) and (19) in the proposed method.

Table II
Experimental verification of coils' self-resonant frequency

Coil	Coil Parameters	Measured f_{self}	Predicted f_{self}
A	L=924uH, D_{out}=36mm, D_{in}=28mm, b=5mm, N_t=150, N_s=*30*	1.2MHz	1.3MHz
B	L=111uH, D_{out}=40mm, D_{in}=28mm, b=5mm, N_t=50, N_s=*150*	2.4MHz	2.9MHz
C	L=69uH, D_{out}=40mm, D_{in}=32mm, b=5mm, N_t=37, N_s=*150*	3.3MHz	3.5MHz
D	L=60uH, D_{out}=20.2mm, D_{in}=18mm, b=0.5mm, N_t=40, N_s=*4*	7MHz	6.1MHz
E	L=45uH, D_{out}=22mm, D_{in}=18mm, b=0.5mm, N_t=34, N_s=*7*	3.9MHz	3.6MHz

Results from Table II demonstrate that the proposed analytical model is accurate in calculating the self-resonant frequency of multiple-layer coils.

VI. Conclusions

A model for calculating the self-resonant frequency of the coil is proposed and the analytical equation is obtained. Using the equation, self-resonant frequency can be calculated given the coil's geometry parameters and winding sequence. Practical guidelines to improve the coil's self-resonant frequency are also given. The calculation results have been validated and they are agreeable with the experimental measurement ones.

Acknowledgement

This work is partially supported by the funding provided by NSF through BMES-ERC.

Reference

[1] W. Liu, et al., "A Neuro-Stimulus Chip with Telemetry Unit for Retinal Prosthetic Device," *IEEE J. Solid-State Circuits*. vol. 35, pp. 1487-97, Oct. 2000.

[2] H. McDermott, "An advanced multiple channel cochlear implant," *IEEE Trans. on Biomed. Eng.*, vol. 36, pp. 789 – 797, July 1989.

[3] P. N. Murgatroyd, "Calculation of proximity losses in multistranded conductor bunches," *IEEE Proc., vol.* 36, pp. 115- 120, 1989

[4] J. A. Ferreira, "Analytical computation of ac resistance of round and rectangular litz wire windings," *Proc. Inst. Elect. Eng*., vol. 139, pp. 21–25, Jan. 1992.

[5] C. R. Sullivan, "Optimal choice for number of strands in a litz-wire transformer winding," *IEEE Trans. Power Electron*., vol. 14, pp. 283–291, Mar. 1999.

[6] L. Theogarajan, et al., "Minimally invasive retinal prosthesis," IEEE *International Solid-State Circuits Conference* pp. 54-55. Feb. 2006.

[7] A. Massarini, M. K. Kazimierczuk, and G. Grandi, "Lumped parameter models for single- and multiple-layer inductors," *IEEE Proc.*, pp. 295–301, June 1996.

[8] A. Massarini and M. K. Kazimierczuk, "Self-capacitance of inductors," *IEEE Trans. Power Electron.*, vol. 12, pp. 671–676, Jul. 1997.

[9] G. A. Kendir, et al., "An Optimal Design Methodology for Inductive Power Link with Class-E Amplifier," *IEEE Transactions on Circuits and Systems – I*, vol. 52, no. 5, pp. 857 – 866, May 2005.

[10] M. N. O. Sadiku, *Elements of Electromagnetics*. Orlando, FL: Sounders College Press, 1994.

[11] F. Grover, *Inductance Calculations: Working Formulas and Tables.* New York: Dover, 1962.

[12] R. C. Dorf, *The Electrical Engineering Handbook,* CRC Press, Boca Raton, 1993.